Superstructure MOF as A Framework to Composite MoS_2 with rGO for Li/Na-ion Batteries Storage with High-performance and Stability

Lei Xu[1], Zhipeng Gong[1], Yinglin Qiu[1], Wenbo Wu[1], Zunxian Yang*[1,2], Bingqing Ye[1], Yuliang Ye[1], Zhiming Cheng[1], Songwei Ye[1], Zihong Shen[1],Yuanqing Zhou[1], Qiaocan Huang[1], Zeqian Hong[1], Zongyi Meng[1], Zhiwei Zeng[1], Hongyi Hong[1], Qianting Lan[1], Tailiang Guo[1,2], Sheng Xu[1,2]

[1]National & Local United Engineering Laboratory of Flat Panel Display Technology, Fuzhou University, Fuzhou 350108, P. R. China.

[2]Mindu Innovation Laboratory, Fujian Science & Technology Innovation Laboratory For Optoelectronic Information of China, Fuzhou,350108, P.R. China

Supporting Information

Captions

Fig.S1 MOF framework Preparation flow chart.

Fig.S2 EDS spectrum of Fe_7S_8-C/ZnS-C@MoS_2/rGO.

Fig.S3 SEM of initial MOF magnifications.

Fig.S4 SEM images of coated MoS2, **(b)** SEM images of coated rGO.

* Corresponding author should be addressed. Tel.: +86 591 8789 3299; Fax: +86 591 8789 2643
E-mail: yangzunxian@hotmail.com (Z. Yang)

Table S1 EDX Smart Quant Results.

Fig.S5 XRD pattern of pure Fe-MOF and Fe,Zn-MOF.

Fig.S6 XPS spectra of N 1s.

Fig.S7 Cycling performance of Fe_7S_8-C/ZnS-C@MoS_2/rGO, Fe_7S_8-C/ZnS-C@MoS_2, and Fe_7S_8-C/ZnS-C@ rGO electrodes at 1 Ag^{-1} and the corresponding Coulombic efficiency of Fe_7S_8-C/ZnS-C@MoS_2/rGO.

Fig.S8 Cycling performance of Fe_7S_8-C/ZnS-C@MoS_2/rGO, electrodes at 5 Ag^{-1}.

Fig.S9 Initial five CV cycles of **(a)** Fe_7S_8-C/ZnS-C@MoS_2 and **(b)** Fe_7S_8-C/ZnS-C@ rGO at 0.5 mVs^{-1} for Li-battery.

Fig.S10 (a) CV curves of the Fe_7S_8-C/ZnS-C@MoS_2 electrode for Li-battery at various scan rates ranging from 0.2 to 1 mVs^{-1} and **(b)** corresponding log(i) versus log(v) plots at peaks I and II. **(c)** CV curve with the pseudocapacitive contribution (the red region) at a scan rate of 0.8 mVs^{-1}. **(d)** Capacitive contribution (in percentage) at different scan rates.

Fig.S11 (a) CV curves of the Fe_7S_8-C/ZnS-C@rGO electrode for Li-battery at various scan rates ranging from 0.2 to 1 mVs^{-1} and **(b)** corresponding log(i) versus log(v) plots at peaks I and II. **(c)** CV curve with the pseudocapacitive contribution (the red region) at a scan rate of 0.8 mVs^{-1}. **(d)** Capacitive contribution (in percentage) at different scan rates.

Fig.S12 Initial five CV cycles of (a) Fe_7S_8-C/ZnS-C@MoS_2 and (b) Fe_7S_8-C/ZnS-C@ rGO at 0.5 mVs^{-1} for Na-battery.

Fig.S13 (a) CV curves of the Fe_7S_8-C/ZnS-C@MoS_2 electrode for Na-battery at

various scan rates ranging from 0.2 to 1 mVs^{-1} and **(b)** corresponding log(i) versus log(v) plots at peaks I and II. **(c)** CV curve with the pseudocapacitive contribution (the red region) at a scan rate of 0.8 mVs^{-1}. **(d)** Capacitive contribution (in percentage) at different scan rates.

Fig.S14 (a) CV curves of the Fe_7S_8-C/ZnS-C@rGO electrode for Na-battery at various scan rates ranging from 0.2 to 1 mVs^{-1} and **(b)** corresponding log(i) versus log(v) plots at peaks I and II. **(c)** CV curve with the pseudocapacitive contribution (the red region) at a scan rate of 0.8 mVs^{-1}. **(d)** Capacitive contribution (in percentage) at different scan rates.

Fig.S15 Cycling performance of Fe_7S_8-C/ZnS-C@MoS_2/rGO electrodes at 0.1 Ag^{-1} for 100 cycles.

Fig.S16 Cycling performance of Fe_7S_8-C/ZnS-C@MoS_2/rGO, Fe_7S_8-C/ZnS-C@MoS_2, and Fe_7S_8-C/ZnS-C@ rGO electrodes at 1 Ag^{-1} and the corresponding Coulombic efficiency of Fe_7S_8-C/ZnS-C@MoS_2/rGO.

Table S2 Comparison of the cycling performance of Fe_7S_8-C/ZnS-C@MoS_2/rGO with the relevant anode materials for Li-ion batteries in the recently reported literature.

Table S3 Comparison of the cycling performance of Fe_7S_8-C/ZnS-C@MoS_2/rGO with the relevant anode materials for Na-ion batteries in the recently reported literature.

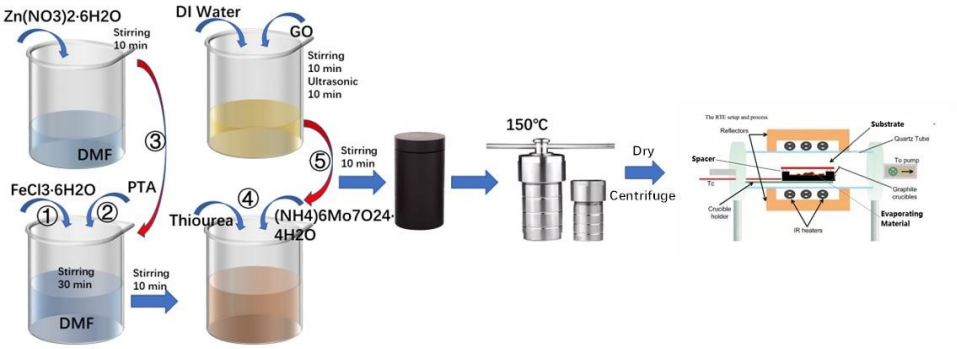
Zn(NO3)2·6H2O
Stirring
10 min
DMF
③
DI Water
GO
Stirring
10 min
Ultrasonic
10 min
⑤
Stirring
10 min
FeCl3·6H2O
PTA
①
②
Stirring
30 min
DMF
Stirring
10 min
④
Thiourea
(NH4)6Mo7O24·
4H2O
150°C
Dry
Centrifuge
Substrate
Reflectors
Quartz Tube
Spacer
To pump
Graphite
crucibles
Crucible
holder
IR heaters
Evaporating
Material

Fig.S1

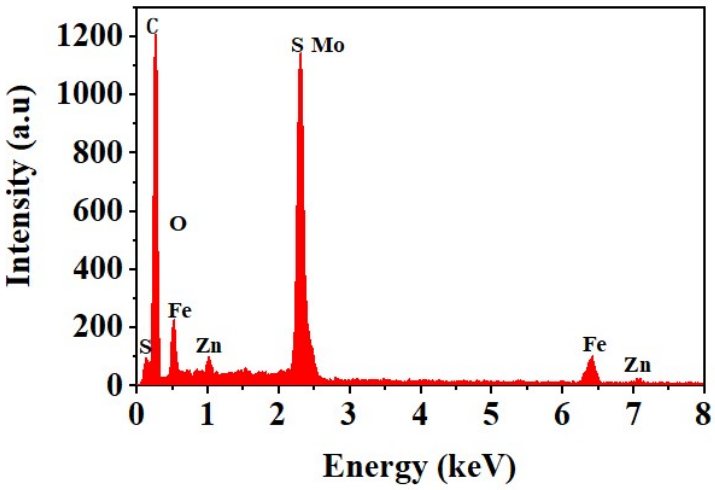
Intensity (a.u)
Energy (keV)
C
O
S Mo
Fe
Zn
S
Fe
Zn
0
200
400
600
800
1000
1200
0
1
2
3
4
5
6
7
8

Fig.S2

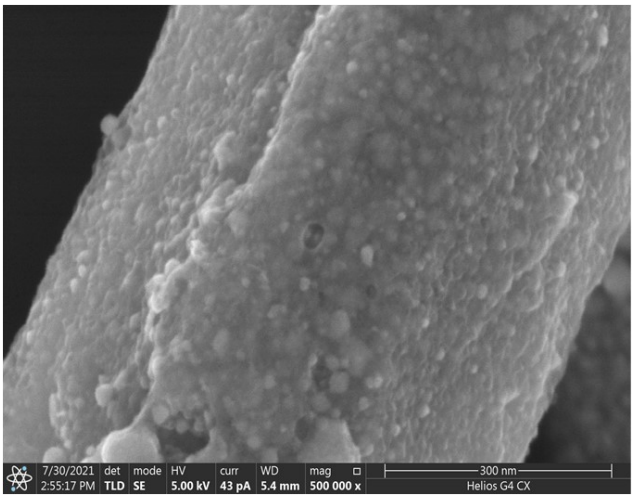
7/30/2021
2:55:17 PM
det
TLD
mode
SE
HV
5.00 kV
curr
43 pA
WD
5.4 mm
mag
500 000 x
300 nm
Helios G4 CX

Fig.S3

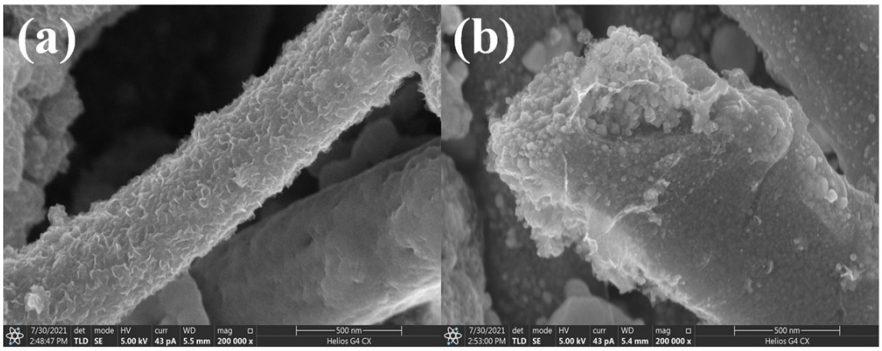
(a)
(b)
7/30/2021 det mode HV curr WD mag
2:48:47 PM TLD SE 5.00 kV 43 pA 5.5 mm 200 000 x
500 nm
Helios G4 CX
7/30/2021 det mode HV curr WD mag
2:53:00 PM TLD SE 5.00 kV 43 pA 5.4 mm 200 000 x
500 nm
Helios G4 CX

Fig.S4

Table S1

Element	Weight	Atomic
C	55.99	9.92
O	7.15	14.29
Zn	1.56	17.26
Mo	13.08	4.82
S	13.25	3.18
Fe	8.97	8.36

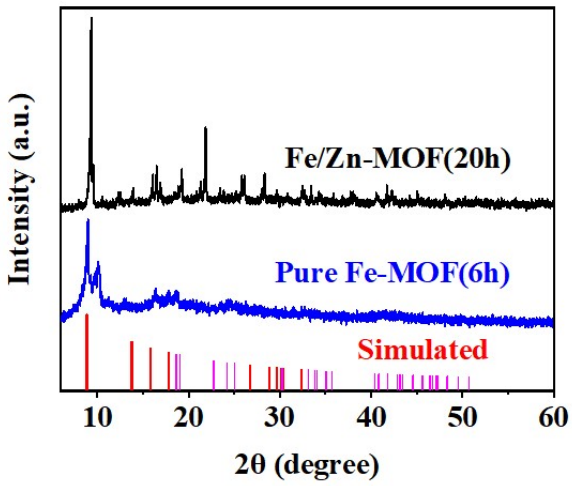
Intensity (a.u.)
Fe/Zn-MOF(20h)
Pure Fe-MOF(6h)
Simulated
10
20
30
40
50
60
2θ (degree)

Fig.S5

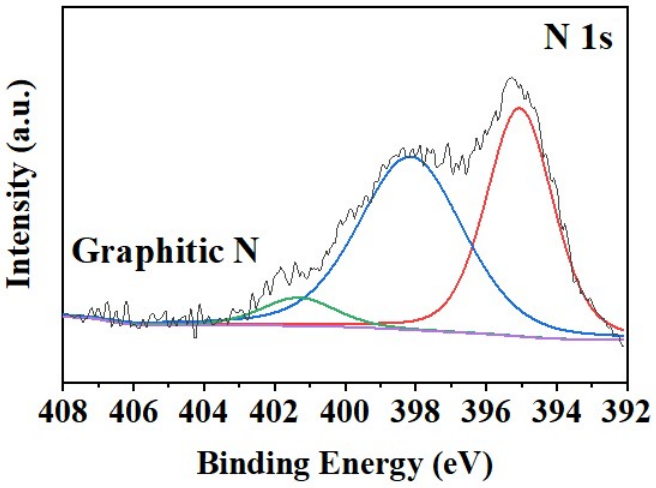
N 1s
Intensity (a.u.)
Graphitic N
408
406
404
402
400
398
396
394
392
Binding Energy (eV)

Fig.S6

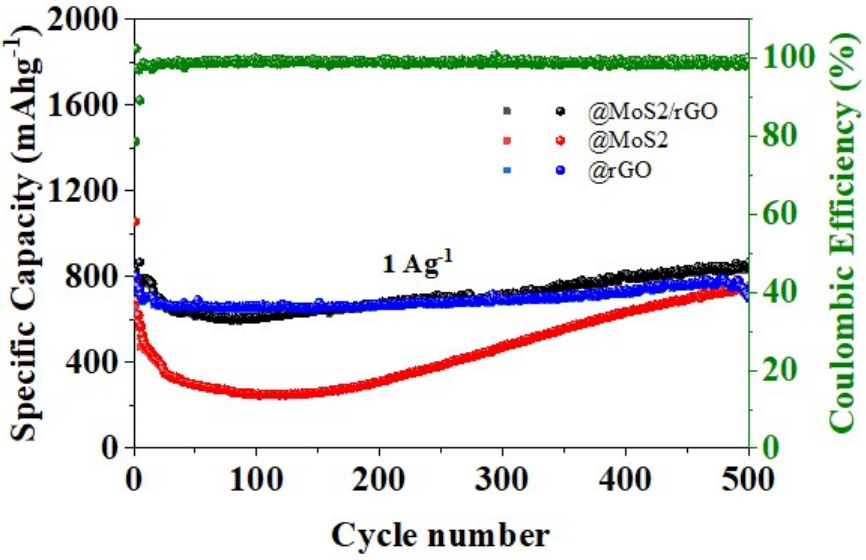
Specific Capacity (mAhg-1)
Coulombic Efficiency (%)
Cycle number
@MoS2/rGO
@MoS2
@rGO
1 Ag-1
0
400
800
1200
1600
2000
0
20
40
60
80
100
0
100
200
300
400
500

Fig.S7

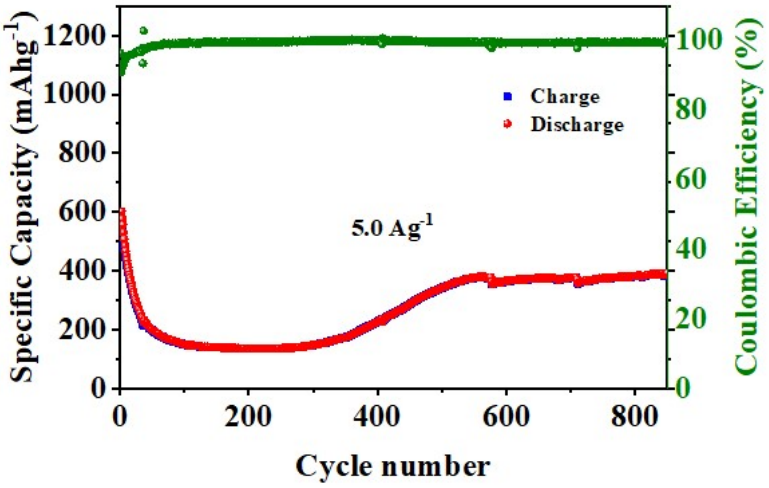
Specific Capacity (mAhg-1)
Coulombic Efficiency (%)
Cycle number
Charge
Discharge
5.0 Ag-1
0
200
400
600
800
1000
1200
20
40
60
80
100

Fig.S8

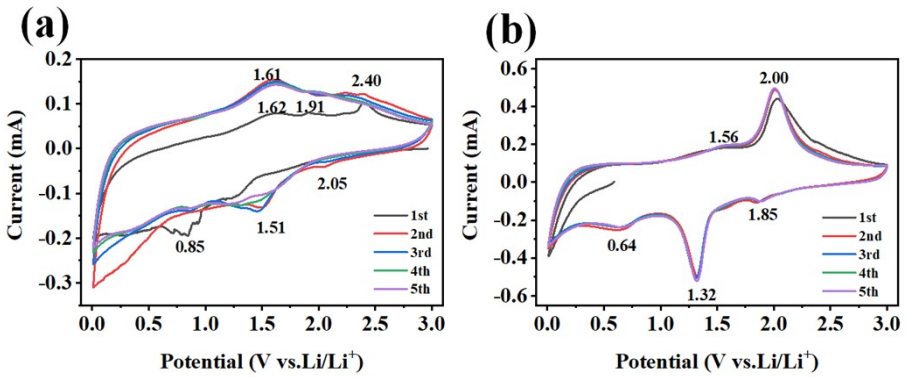
(a)
(b)
Current (mA)
Potential (V vs.Li/Li+)
1.61
2.40
1.62
1.91
2.05
1.51
0.85
2.00
1.56
1.85
0.64
1.32
1st
2nd
3rd
4th
5th

Fig.S9

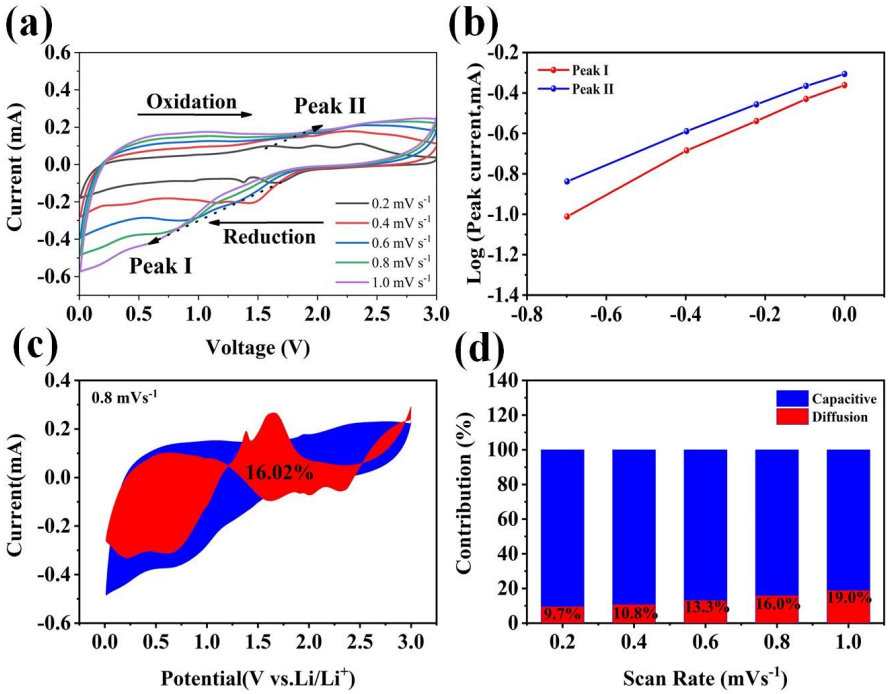
(a)
Oxidation
Peak II
Reduction
Peak I
0.2 mV s-1
0.4 mV s-1
0.6 mV s-1
0.8 mV s-1
1.0 mV s-1
Current (mA)
Voltage (V)
(b)
Peak I
Peak II
Log (Peak current,mA)
(c)
0.8 mVs-1
16.02%
Current(mA)
Potential(V vs.Li/Li+)
(d)
Capacitive
Diffusion
9.7%
10.8%
13.3%
16.0%
19.0%
Contribution (%)
Scan Rate (mVs-1)

Fig.S10

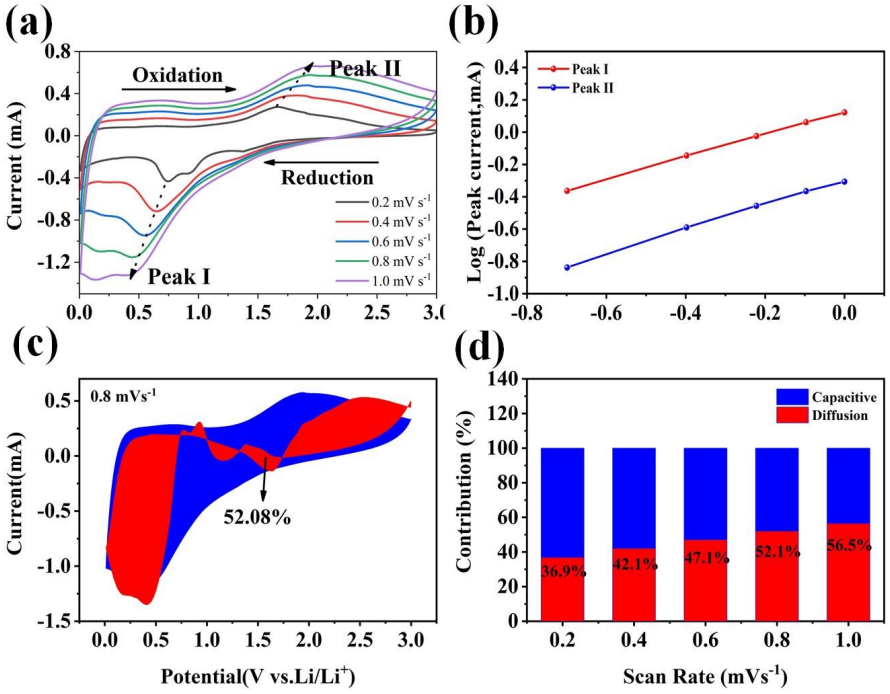
(a)
Oxidation
Peak II
Reduction
Peak I
0.2 mV s-1
0.4 mV s-1
0.6 mV s-1
0.8 mV s-1
1.0 mV s-1
Current (mA)
(b)
Peak I
Peak II
Log (Peak current,mA)
(c)
0.8 mVs-1
52.08%
Current(mA)
Potential(V vs.Li/Li+)
(d)
Capacitive
Diffusion
36.9%
42.1%
47.1%
52.1%
56.5%
Contribution (%)
Scan Rate (mVs-1)

Fig.S11

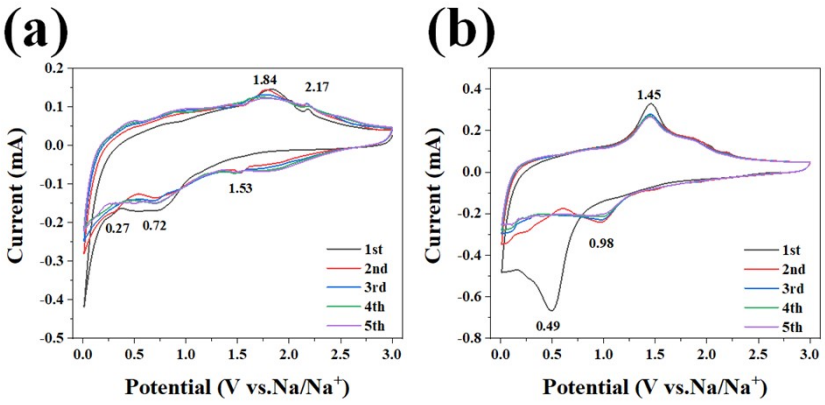
(a)
(b)
Current (mA)
Potential (V vs.Na/Na+)
1.84
2.17
1.53
0.27
0.72
1.45
0.98
0.49
1st
2nd
3rd
4th
5th

Fig.S12

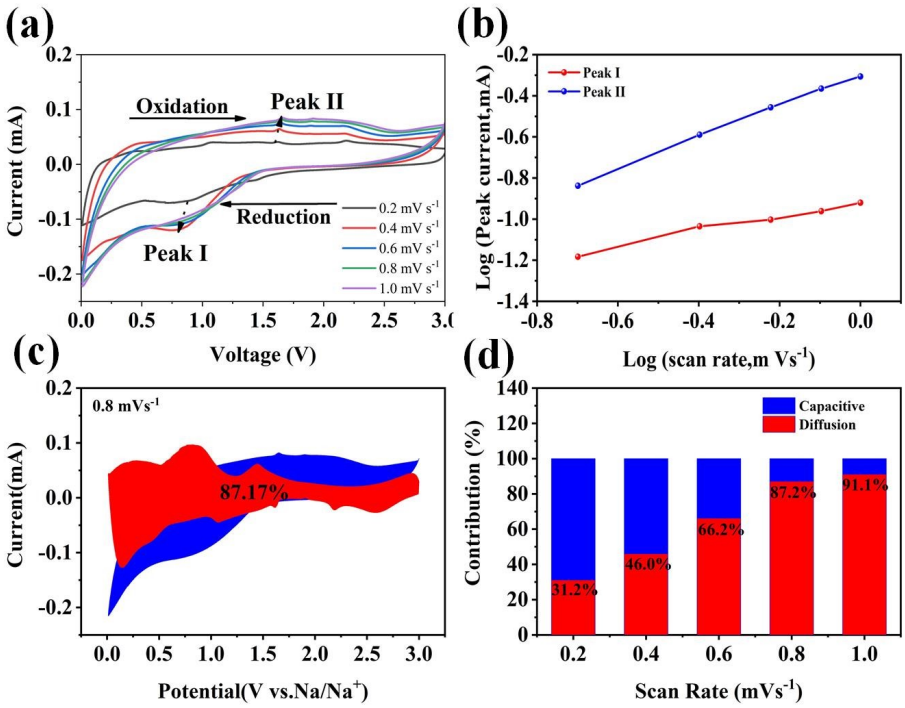
(a)
Oxidation
Peak II
Reduction
Peak I
0.2 mV s-1
0.4 mV s-1
0.6 mV s-1
0.8 mV s-1
1.0 mV s-1
Current (mA)
Voltage (V)
(b)
Peak I
Peak II
Log (Peak current,mA)
Log (scan rate,m Vs-1)
(c)
0.8 mVs-1
87.17%
Current(mA)
Potential(V vs.Na/Na+)
(d)
Capacitive
Diffusion
31.2%
46.0%
66.2%
87.2%
91.1%
Contribution (%)
Scan Rate (mVs-1)

Fig.S13

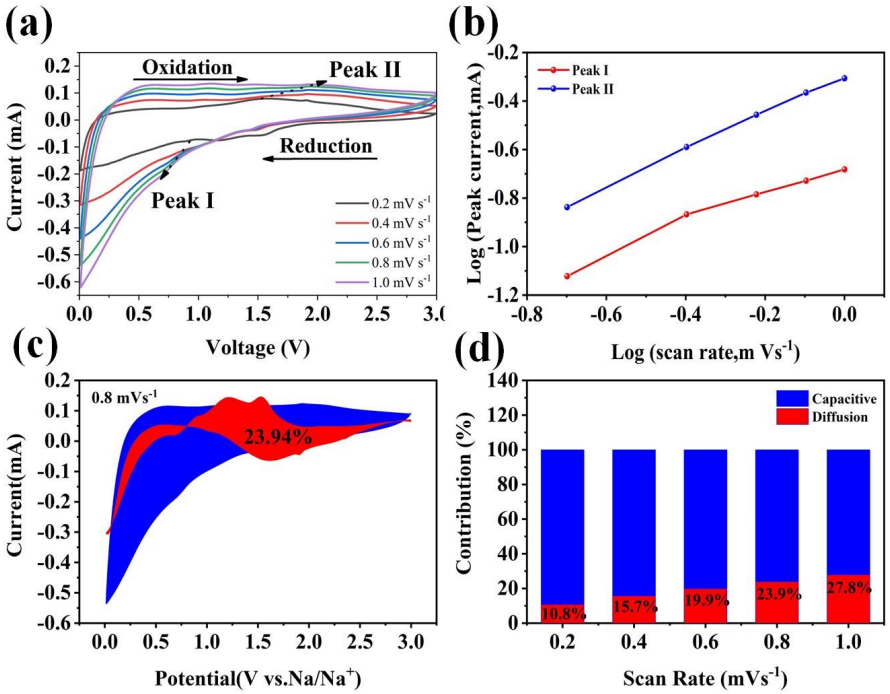
(a)
Oxidation
Peak II
Reduction
Peak I
0.2 mV s-1
0.4 mV s-1
0.6 mV s-1
0.8 mV s-1
1.0 mV s-1
Current (mA)
Voltage (V)
(b)
Peak I
Peak II
Log (Peak current,mA)
Log (scan rate,m Vs-1)
(c)
0.8 mVs-1
23.94%
Current(mA)
Potential(V vs.Na/Na+)
(d)
Capacitive
Diffusion
10.8%
15.7%
19.9%
23.9%
27.8%
Contribution (%)
Scan Rate (mVs-1)

Fig.S14

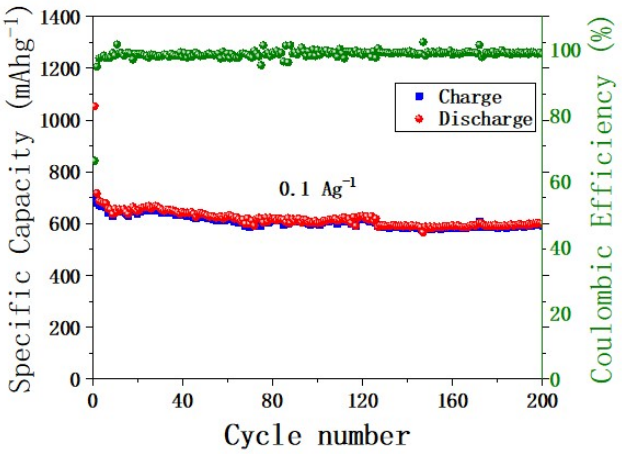
Specific Capacity (mAhg^{-1})
Coulombic Efficiency (%)
Cycle number
Charge
Discharge
0.1 Ag^{-1}
0
200
400
600
800
1000
1200
1400
0
20
40
60
80
100
0
40
80
120
160
200

Fig.S15

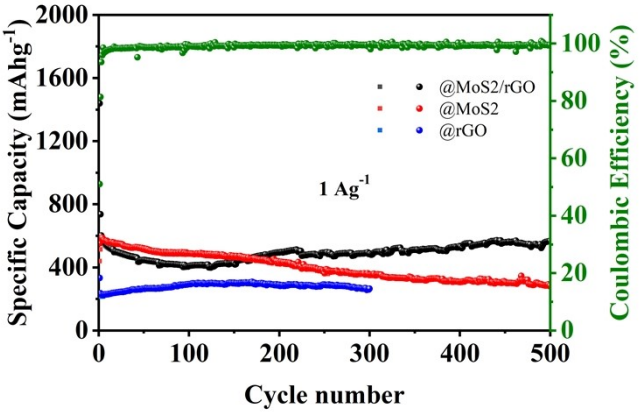
Specific Capacity (mAhg-1)
Coulombic Efficiency (%)
Cycle number
@MoS2/rGO
@MoS2
@rGO
1 Ag-1
0
400
800
1200
1600
2000
0
20
40
60
80
100
0
100
200
300
400
500

Fig.S16

Table S2

MoS_2/C-based anode materials	Current density (mAg^{-1})	(Cycles)	Capacity ($mAhg^{-1}$)	Reference
Fe_7S_8	66	50	110	[1]
Fe_7S_8@NC	100	100	944	[2]
Fe_7S_8@SN-rGO	200 4000	1000 1000	621.1 492.1	[3]
$Fe_{1-x}S$@C	100 0.3	200 40	1185 630	[4]
MoS_2/Carbon	100 2000	200 500	1079 600	[5]
Fe_3O_4/Fe_7S_8@C	100	300	819	[6]
Fe_7S_8-C/ZnS-C@MoS_2/rGO	100 1000 5000	100 500 800	1196.7 866.9 395	This work

Table S3

Fe_7S_8-C/ZnS-C based anode materials	Current density (mAg^{-1})	(Cycles)	Capacity ($mAhg^{-1}$)	Reference
Fe_7S_8@NC	100 2000	50 100	468 415	[2]
$Fe_{1-x}S/MoS_2$	100	100	584.7	[7]
Fe_7S_8@C-G	50	150	449	[8]
M-FeS_2/C	100	200	385	[9]
FeS@C/carbon cloth	91	100	365	[10]
Fe_7S_8-C/ZnS-C@MoS_2/rGO	100	200	592.2	This work

References

[1] X. D. Zheng, Electrochemical characteristics of pyrrhotine as anode material for lithium-ion batteries. **Journal of Alloys and Compounds**, **2016**, **661**: 483-489.

[2] Y. L. Zhou, M. Zhang, Q. Wang, J. Yang, X. Y. Luo, Y. L. Li, R. Du, X. S. Yan, X. Q. Sun, C. F. Dong, X. Y. Zhang, F. Y. Jiang, Pseudocapacitance boosted N-doped carbon coated Fe7S8 nanoaggregates as promising anode materials for lithium and sodium storage. **Nano Research**, **2020**, **13**(3): 691-700.

[3] S. W. Park, H. J. Shin, Y. J. Heo, D. W. Kim, Rational design of S, N Co-doped reduced graphene oxides/pyrrhotite Fe7S8 as free-standing anodes for large-scale, ultrahigh-rate and long-lifespan Li- and Na-ion batteries. **Applied Surface Science**, **2021**, **540**.

[4] C. D. Wang, M. H. Lan, Y. Zhang, H. D. Bian, M. F. Yuen, K. K. Ostrikov, J. J. Jiang, W. J. Zhang, Y. Y. Li, J. Lu, Fe1-xS/C nanocomposites from sugarcane waste-derived microporous carbon for high-performance lithium ion batteries. **Green Chemistry**, **2016**, **18**(10): 3029-3039.

[5] C. H. Wu, J. Z. Ou, F. Y. He, J. F. Ding, W. Luo, M. H. Wu, H. J. Zhang, Three-dimensional MoS2/Carbon sandwiched architecture for boosted lithium storage capability. **Nano Energy**, **2019**, **65**.

[6] H. Tian, Z. G. Wu, Y. J. Zhong, X. S. Yang, X. D. Guo, X. L. Wang, B. H. Zhong, Rapid in-situ fabrication of Fe3O4/Fe7S8@C composite as anode materials for lithium-ion batteries. **Materials Research Bulletin**, **2021**, **133**.

[7] S. Chen, S. Z. Huang, J. P. Hu, S. Fan, Y. Shang, M. E. Pam, X. X. Li, Y. Wang, T. L. Xu, Y. M. Shi, H. Y. Yang, Boosting Sodium Storage of Fe1-xS/MoS2 Composite via Heterointerface Engineering. **Nano-Micro Letters**, **2019**, **11**(1).

[8] C. Z. Zhang, F. Han, J. M. Ma, Z. Li, F. Q. Zhang, S. H. Xu, H. B. Liu, X. K. Li, J. S. Liu, A. H. Lu, Fabrication of strong internal electric field ZnS/Fe9S10 heterostructures for highly efficient sodium ion storage. **Journal of Materials Chemistry A**, **2019**, **7**(19): 11771-11781.

[9] N. Voronina, H. Yashiro, S. T. Myung, Marcasite iron sulfide as a high-capacity electrode material for sodium storage. **Journal of Materials Chemistry A**, **2018**, **6**(35): 17111-17119.

[10] X. Wei, W. H. Li, J. A. Shi, L. Gu, Y. Yu, FeS@C on Carbon Cloth as Flexible Electrode for Both Lithium and Sodium Storage. **Acs Applied Materials & Interfaces**, **2015**, **7**(50): 27804-27809.